The phenomenon of scaling in quasielastic lepton-nucleus scattering. A study of (e, e') and (ν, μ) processes in the relativistic impulse approximation

J.A. Caballero

Departamento de Física Atómica, Molecular y Nuclear, Universidad de Sevilla,
41080 Sevilla, Spain

Abstract. The phenomenon of superscaling for quasielastic lepton induced reactions at energies of a few GeV is investigated in the relativistic impulse approximation. Scaling is shown to emerge from the analysis of electron and charged-current neutrino reactions on nuclei. The experimental scaling function presents an asymmetric shape which is reproduced by the model when final state interactions are accounted for through the relativistic mean field approach. Electromagnetic and weak processes lead to a similar superscaling function which supports the universality property of scaling phenomenon.

1 The phenomenon of scaling in (e, e') processes. Antecedents and general aspects

The phenomenon of scaling occurs in diverse fields in Physics: solid state, atomic, molecular, nuclear, high-energy physics. Scaling in scattering experiments is directly linked to processes where a weakly interacting projectile scatters from a composite system. This is the case, for instance, of electron scattering (with energies of the order of KeV) from electrons bound in atoms, scattering of thermal neutrons from atoms in solids or liquids, and scattering of GeV electrons or muons from quarks in nucleons and nuclei. Despite the extraordinary range of transferred energy and momentum involved in these reactions, the conceptual bases used to describe the scaling phenomena in these different fields have many features in common.

In a general process where a projectile scatters from a complex many-body system, the concept of scaling emerges when the response of the complex system does not longer depend on two independent variables, the energy ω and momentum q transferred in the process, but only on a particular combination of those, called the scaling variable. The functional independence of the complex system response with the transfer momentum q (which sets the scale in the process) is seen as a signature that the scattering occurs between the projectile and the basic constituents in the target. The interest of scaling concerns two main aspects: i) the existence of scaling gives us direct information on the specific reaction mechanism involved in the scattering process considered, and ii) the scaling function is closely linked to the spectral function corresponding to the constituents in the composite target system.

Perhaps, the most well known process in Physics where scaling is observed corresponds to deep inelastic scattering (DIS) of electrons from nucleons and nuclei. In the asymptotic regime, the hadron structure functions only depend on a single variable, named Bjorken x-variable, given by $x \equiv |Q^2|/2m_N\omega$ with $Q^2 = \omega^2 - q^2$ the transfer four-momentum and m_N the nucleon mass. The independence of the nucleon structure functions with q is known as x-scaling and leads to the description of the scattering process as incoherent elastic scattering between the incident lepton and point-like contituents in the nucleon ("quarks").

In this work our interest is focused on the phenomenon of y-scaling occurring for quasielastic (QE) electron scattering on nuclei at intermediate to high values of the transferred momentum q. For inclusive (e, e') processes, the response functions depend in general on the transfer energy ω and transfer momentum q. However, for high enough values of q, $q \geq 500$ MeV/c, the nuclear response depends only on the variable $y(q, \omega)$ which is the minimum value of the missing momentum p allowed by energy-momentum conservation. This is illustrated in Fig. 1 where we present, for q and ω fixed, the kinematically allowed region for the excitation energy $\mathcal{E} = \sqrt{M_{A-1}^2 + p^2} - \sqrt{(M_{A-1}^0)^2 + p^2}$ compatible with energy-momentum conservation. It is important to point out that the kinematic relations implied by Fig. 1 do not depend on the dynamical model selected beyond the assumption of nucleon knockout.

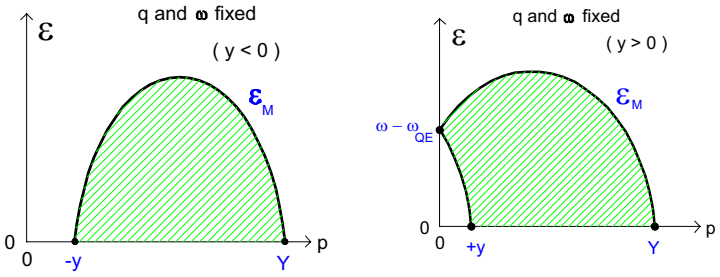

Figure 1. Integration region in the $(\mathcal{E}, p)$ plane for q, ω-fixed.

In order to understand better the significance of the scaling function, let us consider the Plane Wave Impulse Approximation (PWIA). In the PWIA, it is assumed that the knockout nucleon does not interact with the residual nuclear system, i.e., final state interactions (FSI) are neglected. Moreover, negative energy components in the bound nucleon wave function are projected out. Thus, the exclusive $(e, e'N)$ cross section factorizes into a single-nucleon cross section σ^{eN} which takes care of the γNN vertex and the spectral function $S(p, \mathcal{E})$ which contains the whole dependence on the nuclear structure. Then, the inclusive QE (e, e') cross section can be written as an integral over all final states of the exclusive $(e, e'N)$ cross sections for

both proton and neutron knock-out [1]:

$$\left[\frac{d\sigma}{d\epsilon' d\Omega'}\right]_{(e,e')} = \sum_{i=1}^{A} \int_{-y(q,\omega)}^{Y(q,\omega)} pdp \int_{0}^{\mathcal{E}_M(q,\omega;p)} d\mathcal{E} \times \int_{0}^{2\pi} d\phi_N \left(\frac{E_N}{qp_N^2}\right) \left[\frac{d\sigma}{d\epsilon' d\Omega' dp_N d\Omega_N}\right]_{(e,e'N)} . \quad (1)$$

In PWIA and assuming the spectral function to be isospin independent and the single-nucleon cross section $\sigma^{eN}(q,\omega,p,\mathcal{E},\phi_N)$ to be mildly dependent on p and $\mathcal{E}$ (this can be proved), we can finally write,

$$\left[\frac{d\sigma}{d\Omega' d\omega}\right]_{(e,e')} \approx \overline{\sigma}_{eN}(q,\omega;p=-y,\mathcal{E}=0)\cdot F(q,y) \quad (2)$$

where $\overline{\sigma}_{eN}(q,\omega;p=-y,\mathcal{E}=0)$ is the relevant single-nucleon cross section evaluated at fixed values of $\mathcal{E}$ and p, weighted by the corresponding proton and neutron numbers and integrated over the azimuthal ejected nucleon ϕ_N angle. The function $F(q,y) \equiv 2\pi \int_{-y(q,\omega)}^{Y(q,\omega)} pdp \int_0^{\mathcal{E}_M(q,\omega;p)} d\mathcal{E} S(p,\mathcal{E})$ is the scaling function which contains direct information on the spectral function and/or momentum distribution.

Guided by the simple PWIA result, we proceed by defining the experimental scaling function as follows,

$$F(q,y) = \frac{[d\sigma/d\omega d\Omega']_{exp}}{\overline{\sigma}_{eN}(q,\omega;p=-y,\mathcal{E}=0)} \quad (3)$$

Results are shown in Fig. 2 for ^{4}He (left panel) and ^{56}Fe (right panel). As observed, $F(q,y)$ does only show a very mild dependence on q in the region of negative y-values (below the QE peak). In other words, at high enough values of q one seeks the y-scaling behavior: namely, if the inclusive response scales, then F becomes only a function of y, i.e., $F(q,y) \longrightarrow F(y) \equiv F(\infty,y)$. For $y > 0$ (above the QE peak) scaling behavior breaks down due to the presence in this region of nucleon resonances, meson production, etc.

The phenomenon of scaling can be also approached from a different point of view using as a starting point the Relativistic Fermi Gas (RFG) model [2–4]. In spite of its simplicity, the RFG presents some clear advantages: it is fully relativistic, it respects Gauge invariance and it can be solved analytically providing expressions for the nuclear tensor and response functions. The RFG model leads to a universal (valid for all nuclei) scaling function $f_{RFG}(\psi)$ which only depends on the scaling variable $\psi = \frac{y}{k_F}[1+\mathcal{O}(\eta_F^2)]$ with $\eta_F \equiv k_F/m_N$ and k_F the Fermi momentum. Then, we proceed by subtracting from the experimental cross section and experimental response functions the single-nucleon contribution evaluated within the RFG model. In this way, we define the experimental superscaling function $f_{exp}(q,\psi)$, as well as its longitudinal $f_{exp}^L(q,\psi)$ and transverse $f_{exp}^T(q,\psi)$ contributions. Scaling of the first kind emerges if $f_{exp}(q,\psi) \stackrel{q\to\infty}{\longrightarrow} f_{exp}(\psi)$. Scaling of the second kind

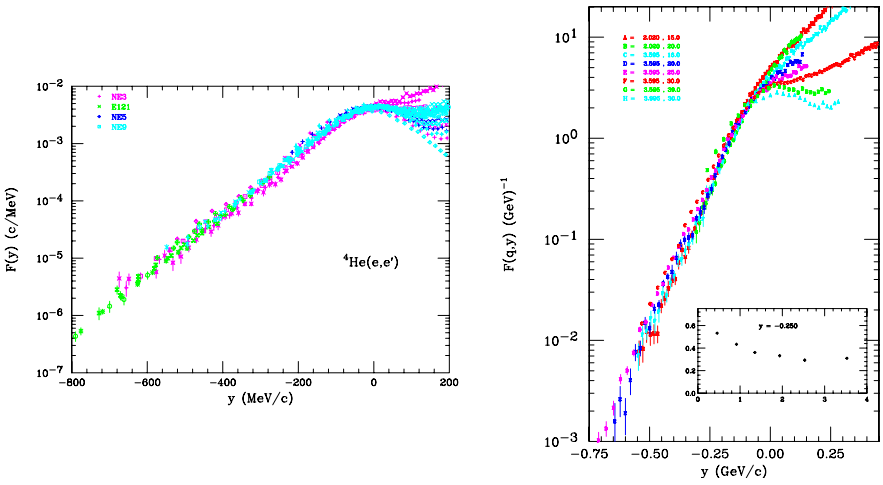

Figure 2. Experimental scaling function $F(q,y)$ for ^{4}He (left) and ^{56}Fe (right).

is satisfied if the function $f_{exp}(\psi)$ does not depend on the nuclear system considered. The simultaneous occurrence of both kinds of scaling is named superscaling. Finally, scaling of the zeroth kind refers to $f_{exp}(q,\psi) = f^L_{exp}(q,\psi) = f^T_{exp}(q,\psi)$.

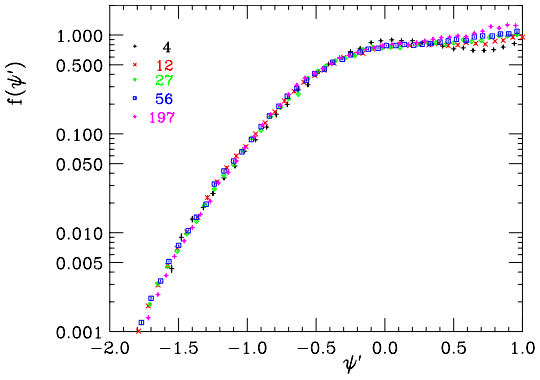

Figure 3. Function $f(\psi)$ for nuclei $A = 4 - 197$ and fixed kinematics ($q \approx 1000$ MeV/c).

In Fig. 3 we show $f_{exp}(\psi)$ for different nuclei, whereas in Fig. 4 $f^L_{exp}(\psi)$ (left panel) and $f^T_{exp}(\psi)$ (right) are presented. ¿From all of these results one concludes that scaling of the first kind is reasonable below the QE peak ($\psi \leq 0$), whereas scaling of the second kind is excellent in the same region. On the contrary, breaking of scaling, particularly of the first kind, is observed above the QE peak ($\psi \geq 0$). This is due to effects beyond the Impulse Approximation (IA), mainly in the transverse channel. Finally, the longitudinal response superscales. All these results are

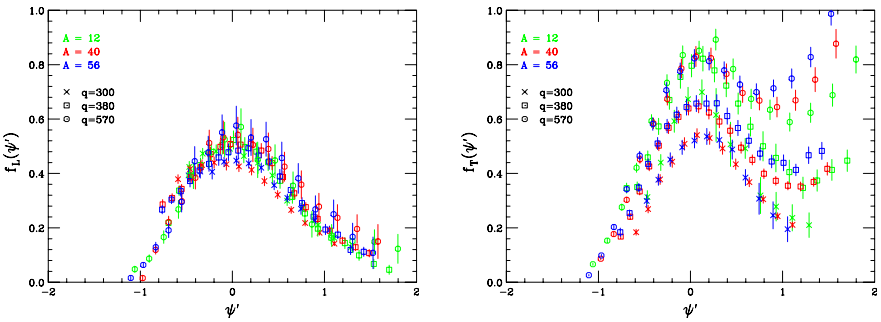

Figure 4. Scaling function $f_L(\psi)$ (left panel) and $f_T(\psi)$ (right).

summarized in Fig. 5 where the experimental superscaling function extracted from the analysis of the longitudinal (e, e') world data is shown and it is compared with the RFG curve. As observed, the experimental function presents a clear asymmetric shape with a long tail extended to positive ψ-values. These results constitute a strong constraint for any theoretical model describing QE electron scattering processes (see [2–4] for more details).

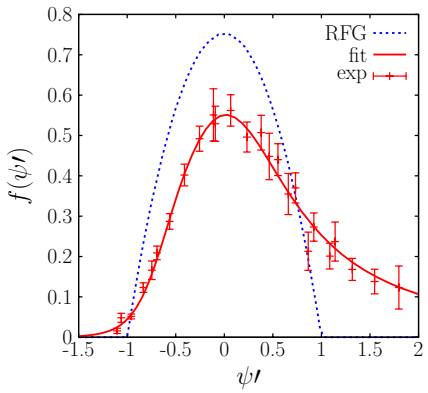

Figure 5. Averaged $f_L(\psi)$ together with a parametrization (solid) and RFG result (dashed).

2 The model: Relativistic Impulse Approximation and Final State Interactions

Within the Relativistic Impulse Approximation (RIA), the many-body nuclear current operator is simply given as a sum of single-nucleon current operators that only couple the target ground state to scattering states lying in the one-body knockout

space. Bound nucleon wave functions are given as self-consistent Dirac-Hartree solutions, whereas the outgoing nucleon state is described as a relativistic scattering wave function. Here, different approaches have been considered to account for final state interactions: i) use of the phenomenological relativistic optical potential, but with the imaginary part set to zero (this is denoted as rROP), ii) use of distorted wave functions obtained with the same relativistic mean field used to describe the initial bound nucleon states (denoted RMF), and iii) neglect FSI, i.e., the outgoing nucleon is simply described as a free relativistic Dirac wave function (RPWIA). Concerning the current operator, we use the relativistic free nucleon expressions denoted as CC1 and CC2 (see [5–7] for details on the RIA model).

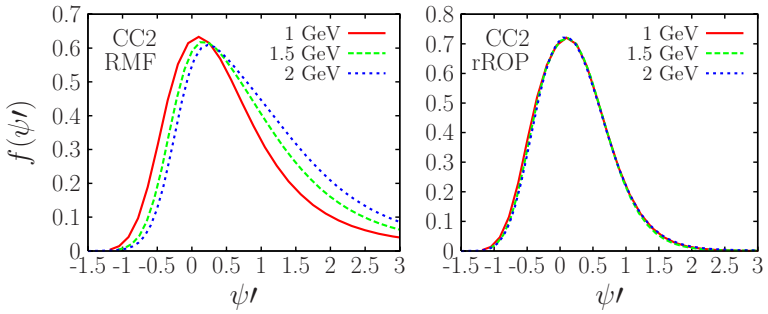

Figure 6. Analysis of first kind scaling. Scaling functions for different values of the incident electron energy. Results correspond to RMF (left panel) and rROP (right) descriptions of FSI.

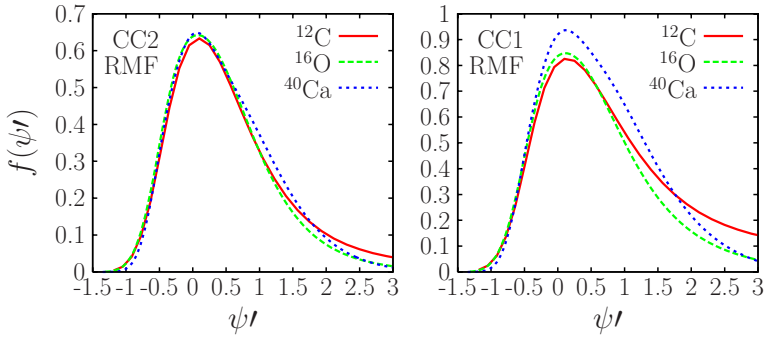

Figure 7. Analysis of second kind scaling. Scaling functions for three nuclei. Results correspond to CC2 (left) and CC1 (right) nucleon operators and RMF-FSI description.

In Figs. 6 and 7 we present the RIA analysis for the first and second kind scaling, respectively. In the first case, the CC2 operator [8] has been selected and results for RMF (left panel) and rROP (right panel) descriptions of FSI are shown. As noticed, a shift in $\psi' < 0$ is observed for RMF and breakdown of scaling occurs at roughly

$\sim 25-30\%$ for $\psi' > 0$ (this is compatible with data). On the contrary, scaling of the first kind is excellent in the rROP approach (likewise for RPWIA). In Fig. 7, both current operators, CC2 (left panel) and CC1 (right) have been considered within the RMF description of FSI. Results show that scaling of the second kind is excellent for the CC2 operator, whereas a visible scaling violation occurs for CC1 (mainly due to the T contribution). To conclude, we add also some comments concerning scaling of the zeroth kind, i.e., $f_L(\psi) = f_T(\psi) = f(\psi)$. This property emerges from RFG (by construction), and it is also verified within RPWIA and non-relativistic (NR) or semi-relativistic (SR) approaches for different FSI descriptions [9, 10]. On the contrary, the fully relativistic approach implied by the RMF model leads to a visible violation of the zeroth kind scaling property which is directly linked to the role played by relativistic nuclear dynamics in the final channel in presence of strong relativistic potentials [11].

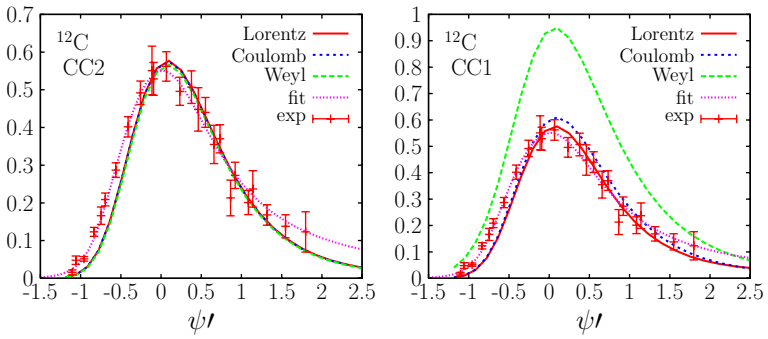

Figure 8. Longitudinal $f_L(\psi)$ function evaluated for three gauges and the two current operators. RMF description of FSI and comparison with data.

In Fig. 8 the RIA-RMF $f_L(\psi)$ curve is presented and it is compared with the analysis of longitudinal (e, e') world data. Results corresponding to rROP and RPWIA approaches lead to symmetrical scaling functions that do not fit experiment. Fig. 8 shows also that only the CC2+RMF approach leads to a function $f_L(\psi)$ which is almost independent on the gauge selected fulfilling the Coulomb sum rule: $\int d\psi f_L(\psi) \approx 1$.

The basic conclusions can be summarized as follows: i) superscaling shows up in RIA calculations, even in presence of very strong potentials (rROP & RMF), ii) description of FSI through the RMF model leads to a function $f(\psi)$ with the right asymmetry required by the experiment, and iii) breaking of scaling is clearly observed when FSI are present and the CC1 current operator is used.

3 Scaling applied to neutrino-nucleus scattering

We restrict ourselves to the analysis of charge-changing neutrino-nucleus scattering reactions, (ν_μ, μ). Notice that the kinematics involved in (ν, μ) is similar to (e, e'); namely, the final lepton is assumed to be detected, hence one has control on the energy and momentum transferred in the process. The general formalism for (ν_μ, μ) reactions has been presented in [9, 12]. Here we focus on the QE peak and show results within the RIA model described in the previous section [7]. The single-nucleon weak current is given by $J^\mu_w = J^\mu_V - J^\mu_A$, with J^μ_V the vector current given in terms of the pure isovector nucleon form factors F_1^V and F_2^V, and J^μ_A the axial-vector current which depends on the axial G_A and pseudoscalar G_P nucleon form factors.

The general procedure to apply scaling in neutrino-nucleus scattering makes use of the RFG results. We start by extracting the single-nucleon contribution from the differential (ν, μ) cross section (see [12] for explicit expressions of the single-nucleon weak responses (RFG)). Then, we proceed by reconstructing the neutrino-nucleus cross section using the experimental scaling function extracted from experimental (e, e') data. This means that we assume the scaling function $f(\psi)$ to be universal and therefore, valid for CC (ν_μ, μ) processes. The use of the experimental superscaling function $f_{exp}(\psi)$ in constructing neutrino-nucleus cross sections is known as SuperScaling Analysis (SuSA) and was introduced for the first time in [12].

A different approach to scaling studies in neutrino reactions is based on the use of a specific theoretical model which describes successfully (e, e') data. This is the case of the RIA-RMF model. We evaluate the inclusive (ν, μ) cross section within the RIA and then divide it by the corresponding single-nucleon cross section, weighted by the appropriate proton (Z) and/or neutron (N) numbers. Proceeding in this way we can analyze if the RIA scaling function does satisfy scaling properties. Moreover, we can also determine if the RIA function $f(\psi)$ obtained from (ν, μ) cross sections is consistent with $f(\psi)$ obtained from (e, e') calculations (with the same model). In other words, we can answer the following question: does the RIA model lead to a similar scaling function $f(\psi)$ for (e, e') and (ν, μ) processes?, and if so, how does this function compare with the experimental one $f_{exp}(\psi)$?

The analysis is presented in Fig. 9 where we show results for RPWIA (top panels), rROP (middle) and RMF (bottom). Left panels refer to scaling of the first kind and right panels to the second kind. As observed, results follow similar trends to the ones already shown for (e, e') reactions, that is, scaling of the second kind works in an excellent way, whereas breakdown of scaling of the first kind at some degree is produced within the RMF model (compatible with data). Results in Fig. 10 allow us to analyze the universal character of the scaling function and its validity for electromagnetic and weak interactions. We directly compare the functions $f_L(\psi)$ and $f_T(\psi)$ obtained from (e, e') cross sections with the ones corresponding to (ν_μ, μ^-) and $(\overline{\nu}_\mu, \mu^+)$ reactions. The averaged QE phenomenological function obtained from the analysis of (e, e') data is also included. As observed, the theoretical curve for $f_L(\psi)$ follows the behavior of the data very closely, and this proves the capability of the RIA combined with the RMF potential to describe satisfactorily (e, e')

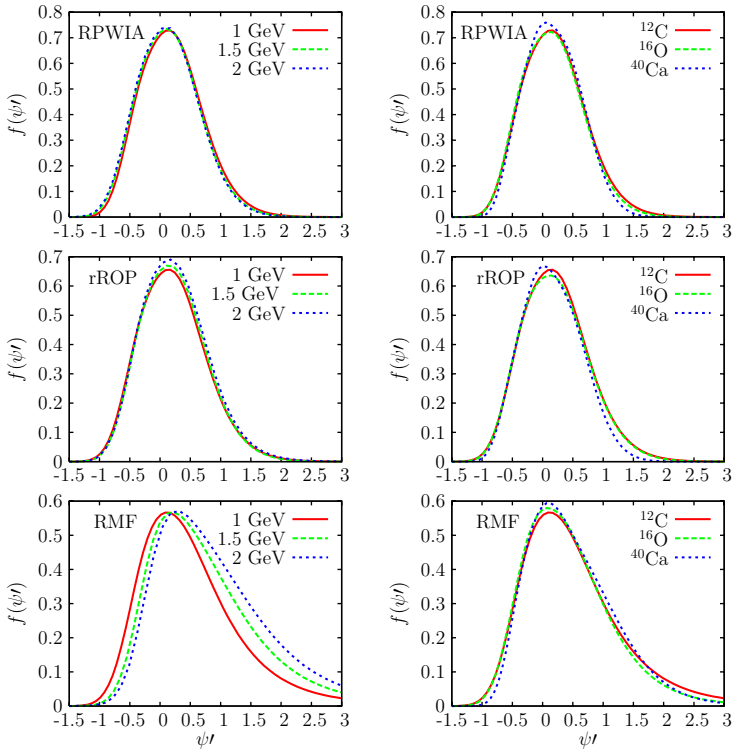

Figure 9. Analysis of the first (left) and second (right) kind scaling for (ν, μ) reactions.

data in the longitudinal channel. On the contrary, the transverse contribution $f_T(\psi)$ overestimates the data by $\sim 20\%$ even in the region close to the maximum, $\psi \approx 0$.

Concerning the scaling function obtained for neutrino (and antineutrino) scattering reactions, one observes that it is much more in accordance with $f_L(\psi')$ and hence with the electron scattering longitudinal data, than with $f_T(\psi')$. This outcome reinforces the validity of the general assumption implied by SuSA [12], i.e., the use of the phenomenological scaling function (extracted from the analysis of longitudinal QE electron scattering data) to predict CC neutrino-nucleus cross sections. However, it is also striking that $f(\psi')$ for ν_μ and $\overline{\nu}_\mu$ reactions, which are totally dominated by the purely *transverse* (T, T') channels, coincides with the f_L function of (e, e') instead of f_T, in contrast to what one might expect.

In order to understand these results, one must be aware of some basic differences between (e, e') and (ν, μ) reactions. In the former, the longitudinal and transverse channels contribute importantly (at least for some kinematics), and in both responses isoscalar and isovector form factors enter. In contrast, only purely isovector form factors enter in CC neutrino-nucleus scattering. In what follows we investigate how the functions f_L and f_T obtained from (e, e') RMF calculations change when the

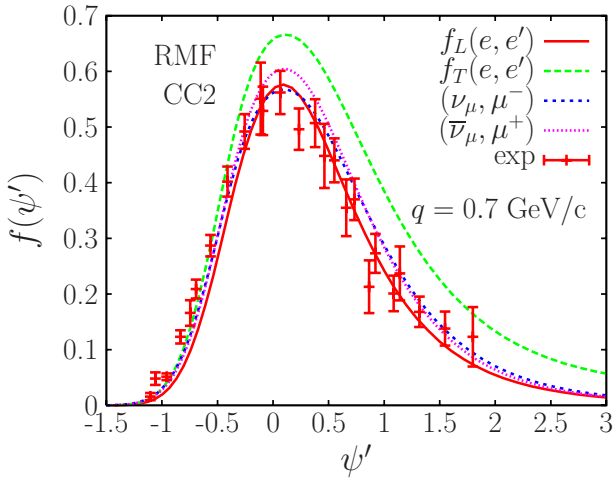

Figure 10. Longitudinal and transverse scaling functions for (e,e') compared with $f(\psi)$ evaluated from neutrino-nucleus scattering. All results correspond to RMF-FSI description and CC2 current operator.

isoscalar form factors are removed. Notice that proceeding in this way, we force the (e,e') to be purely isovector, similar to what occurs for (ν,μ).

The results of our analysis are presented in Fig. 11. Again, we compare the scaling functions f_L and f_T for electrons with those of neutrinos and antineutrinos. Experimental (e,e') data are also included for reference. Top and bottom panels refer to different assumptions concerning the electromagnetic form factors entering in (e,e') reactions. First, the curves f_L and f_T in the top panel have been obtained assuming $G_M^n = -G_M^p$, i.e., we remove the isoscalar contribution in the magnetic form factor which, consequently, becomes purely isovector. The proton and neutron electric form factors are not modified. Therefore, results for (e,e') in the top panel of Fig. 11 reflect the scaling functions where the isoscalar contribution only enters through the electric content of the nucleons. As observed, results in Fig. 11, when compared with Fig. 10, show that the discrepancy between f_L and f_T gets smaller because a visible decrease occurs for f_T. In other words, removing the isoscalar contribution in G_M leads to a weaker violation of the zeroth-kind scaling property (within the RMF context).

In the bottom panel of Fig. 11 we show the results corresponding to no convective terms, i.e., the electric form factors for protons and neutrons (in the electromagnetic sector) are forced to be zero. The reason to consider this non-convective limit comes from the effects introduced by the isoscalar/isovector contributions in the electric form factors of the nucleon. Obviously, the neglect of convective terms yields neither isoscalar nor isovector contributions. While being aware of the important differences introduced in the cross sections due to the assumption $G_E^p = G_E^n = 0$, it is instructive to explore the behavior of the scaling functions in such approximations. The results in the bottom panel of Fig. 11 show that a unique

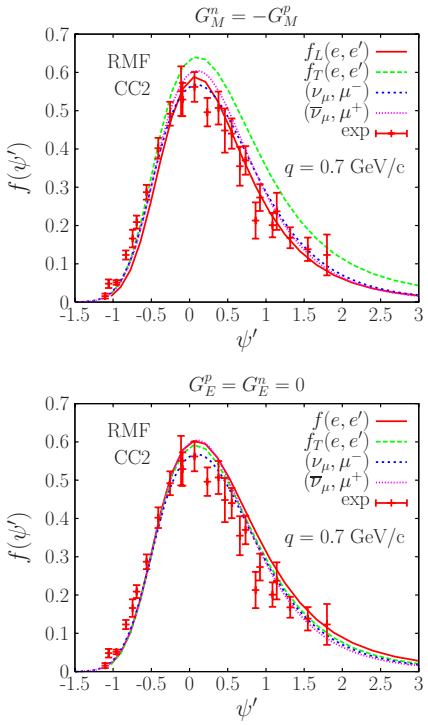

Figure 11. Same as previous figure, but with modified isoscalar/isovector contributions via the nucleon form factors in the (e, e') case.

(*universal*) scaling function emerges from the analysis of (e, e') calculated cross sections. Moreover, this function (without isoscalar terms) agrees with the one evaluated from (ν_μ, μ^-) and $(\overline{\nu}_\mu, \mu^+)$ processes and with $f_{exp}(\psi')$ extracted from the analysis of longitudinal (e, e') world data. Results on integrated (ν, μ) cross sections are given in [13].

We may summarize our basic conclusions in this section as follows: i) superscaling behavior is satisfied by RIA calculations for all FSI descriptions studied, ii) scaling functions obtained from QE (e, e') and (ν, μ) cross sections are rather similar. This result is consistent with the "universal" character of $f(\psi)$, iii) differences between (e, e') and (ν, μ) results obtained within the RIA+RMF model are consistent with the role played by isoscalar and isovector nucleon form factors in the two processes, iv) breaking of zeroth kind scaling and the balance between proton and neutron contributions in the scaling function for (e, e') are proven to be significantly affected by dynamical relativistic effects, mainly in the final state, and v) only the RMF description of FSI leads to an asymmetric scaling function that fits nicely the experimental function extracted from QE (e, e') data.

Acknowledgements

This work was partly supported by DGI (Spain) under Contracts Nos. FIS2005-01105, FPA2006-13806, by the Junta de Andalucía, and by the INFN-CICYT collaboration agreement INFN06-15. This work has been done in collaboration with J.E. Amaro, M.B. Barbaro, T.W. Donnelly, M.C. Martínez, C. Maieron and J.M. Udías. I warmly thank all of them.

References

1. D. B. Day, J. S. McCarthy, T. W. Donnelly and I. Sick, Ann. Rev. Nucl. Part. Sci. **40**, 357 (1990).
2. T.W. Donnelly and I. Sick, Phys. Rev. Lett. **82**, 3212 (1999).
3. T.W. Donnelly and I. Sick, Phys. Rev. C **60**, 065502 (1999).
4. C. Maieron, T.W. Donnelly and I. Sick, Phys. Rev. C **65**, 025502 (2002).
5. J.M. Udías *et al.*, Phys. Rev. C **48**, 2731 (1993); **51**, 3246 (1995); Phys. Rev. Lett. **83** (1999) 5451; **64**, 024614-1 (2001).
6. J.A. Caballero, J.E. Amaro, M.B. Barbaro, T.W. Donnelly, C. Maieron, J.M. Udías, Phys. Rev. Lett. **95**, 252502 (2005).
7. J.A. Caballero, Phys. Rev. C **74**, 015502 (2006).
8. T. de Forest, Nucl. Phys. **A 392**, 232 (1983).
9. J.E. Amaro, M.B. Barbaro, J.A. Caballero, T.W. Donnelly, C. Maieron, Phys. Rev. C **71**, 065501 (2005).
10. J. E. Amaro, M. B. Barbaro, J. A. Caballero, T. W. Donnelly, J.M. Udías, Phys. Rev. C **75**, 034613 (2007).
11. J.A. Caballero, J.E. Amaro, M.B. Barbaro, T.W. Donnelly, J.M. Udías, Phys. Lett. **B 653** (2007) 366.
12. J.E. Amaro, M.B. Barbaro, J.A. Caballero, T.W. Donnelly, A. Molinari and I. Sick, Phys. Rev. C **71**, 015501 (2005).
13. J.E. Amaro, M.B. Barbaro, J.A. Caballero, T.W. Donnelly, Phys. Rev. Lett. **98** (2007) 242501.